論文 96-21-2-10

Performance Evaluation of the Single-Dwell and Double-Dwell Detection Schemes in the IS-95 Reverse Link

Bub-Joo Kang*, Hyung-Rae Park*, Jung-Young Son**
Chang-Eon Kang**, *Regular Members*

IS-95역방향 링크에서 단일 적분 및 이중 적분 검색 방식의 성능 분석

正會員 강 법 주*, 박 형 래*, 손 정 영**, 강 창 언**

ABSTRACT

This paper considers the evaluation of the acquisition performance for an access channel preamble based on a random access procedure of direct sequence code division multiple access(DS/CDMA) reverse link. The parallel acquisition technique that employs the single-dwell detection scheme and the multiple-dwell(double-dwell) detection scheme is mentioned. The acquisition performance for two detection schemes is compared in terms of the acquisition probability and the acquisition time. The parallel acquisition is done by a bank of N parallel I/Q noncoherent correlators. Expressions on the detection, false alarm, and miss probabilities of the single-dwell and multiple-dwell(double-dwell) detection schemes are derived for multiple H_1 cells and multipath Rayleigh fading channel. Comparing the single-dwell detection scheme with the multiple-dwell(double-dwell) detection scheme in the case of employing the parallel acquisition technique in the reverse link, the numerical results show that the single-dwell detection scheme demonstrates a better performance.

요 약

본 논문은 DS/CDMA 역방향 링크의 랜덤 액세스 과정에 근거하여 액세스 채널 프리앰블에 대한 동기 획득 성능을 분석하고 있다. 적용된 동기 획득 기술로는 병렬 동기 획득이며 단일 적분 검출 방식과 다중 적분(이중 적분)

*한국전자통신연구소 이동통신연구단 이동통신방식연구실
Signal processing section, Mobile communication research division, ETRI
**연세대학교 전자공학과
Yonsei University.
論文番號:95237-0711
接受日字:1995년 7월 11일

검출 방식 등이 도입되었다. 두 검출 방식들에 대한 동기 획득 성능은 동기 획득 확률과 동기 획득 시간에 의하여 비교되었다. 병렬 동기 획득은 N개의 병렬 I/Q 넌코히런트 상관기들에 의해 수행되었다. 두 검출 방식들에 대한 신호 검출, 오보, 그리고 miss 확률들은 다수 H_1 셀과 나정로 페이딩 채널에 대하여 유도되었다. 역방향 링크에서 병렬 동기 획득을 적용한 경우, 단일 적분 검출 방식과 이중 적분 검출 방식을 비교하면, 수치 해석 결과는 단일 적분 검출 방식이 보다 더 좋은 성능을 나타냄을 보여주고 있다.

Ⅰ. Introduction

In recent years, DS/CDMA has become more popular in the area of digital cellular and personal communication networks, because it includes the well-known capability to both combat multipath and allow multiple users to simultaneously communicate over a channel, However, advantages of DS/CDMA can be exploited only when the PN code sequence of the receiver and incoming signal are synchronized within a fraction of a pseudonoise(PN) chip. Typically, process of code synchronization is achieved in two steps, the acquisition(coarse alignment) step and the tracking(fine alignment) step [1]. In this paper, the acquisition of the random access signal in the reverse link is mainly mentioned. Since the pilot channel is not utilized for power efficiency of a mobile station in the reverse link, the noncoherent demodulation has been proposed [2]. Considering power efficiency and hardware complexity, searcher and data demodulator can be composed of the I/Q noncoherent correlator.

Because the multiple users use a code channel assigned to the access channel in the case of the random access in the reverse link, the acquisition for the random access signal should be achieved rapidly. Most of the acquisition schemes that have been suggested for minimizing the acquisition time have applied the serial acquisition [3, 4]. In order to realize a fast acquisition, the parallel acquisition that applys a bank of N parallel I/Q noncoherent matched filters(MFs) or a bank of charge-coupled device(CCD) convolvers has been suggested in [5-8].

In this paper, the parallel acquisition technique that uses a bank of N I/Q noncoherent correlators is investigated. The output characteristic of each I/Q noncoherent correlator are analyzed for the band-limited and Rayleigh fast fading channel. The independent fading of all users is also assumed. Based on a fading environments described above, expressions of the detection, false alarm, and miss probabilites are derived. The mean acquisition time for two detection schemes which are proposed is also derived. The purpose of this paper is to examine and compare the parallel acquisition performance of the single-dweel detection scheme and the multiple-dwell(double-dwell) detection scheme. The comparision of the acquisition performance for two detection schemes is mentioned by the acquisition probability for a decision threshold and the sensitivity of the acquisition time to changes in the average random-delay.

This paper is organized as follows. The random access procedure and acquisition systems considered are described in parts A and B of section II, respectively, and the mean acquisition time is derived in part C of section II. The output characteristics of the I/Q noncoherent correlator are analyzed in part A of section III, and expressions of the required probabilities are derived in part B of section III. Numerical results are presented in section IV, and finally, conclusion is discussed in section V.

Ⅱ. System Description

A. Random Access Procedure

The DS/CDMA reverse link consists of the access channel and the reverse traffic channel [9]. The access channel is used for a random access, while the reverse traffic channel is used for communicating user traffic

data. When a mobile station attempts a random access, an access channel slot is utilized. An access channel slot consists of an access channel preamble and an access channel message. An access channel preamble is always spreaded by the PN code sequence of zero code-phase offset. It is also unmodulated by data signal. An access channel message consists of access message and cyclic redundancy code(CRC). The access message is classified by two types of messages: a response message(one that is a response to a base station) or a request message(one that is autonomously by the mobile station).

The random access procedure is briefly described as follows. The timing of the transmission of an access channel slot is determined pseudorandomly. If the initial acquisition is finished within a given access channel preamble, a base station does noncoherent demodulation of M-ary othogonal signals, Viterbi decoding, and CRC checking over an access channel message. If the no error is detected by CRC checking, an access attempt succeeds and a base station's sends an acknowledgement to mobile station. If an acknowledgement is correctly received, an access attempt terminates. But, if the errors are detected by CRC checking, an access attempt fails, and a base station does not send an acknowledgement to a mobile station. In the case of failure of an access attempt, an access channel slot of a specified mobile station is pseudorandomly repeated at the base of the system time, namely, it is retransmitted after the random-delay.

In this paper, in order to facilitate the evaluation of the acquisition performance, the no error is assumed to be detected by CRC checking.

B. Acquisition Model for The Single-Dwell and Double-Dwell Detection Schemes

In the reverse link, since the transmitted signal of the mobile station is spreaded by the PN code sequence of the zero code-phase offset, the uncertainty region is determined by the round-trip delay due to cell radius. Thus, the uncertainty region, V, can be

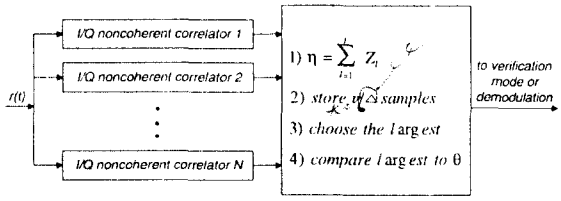

Fig. 1. N parallel I/Q noncoherent correlators for the single-dwell and double-dwell detection schemes

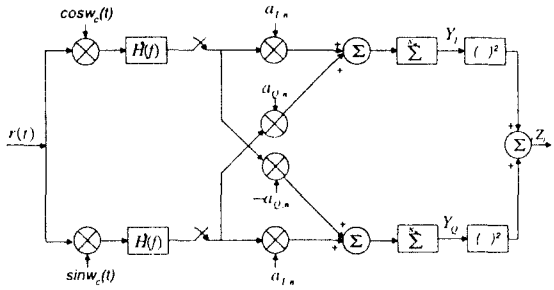

Fig. 2. I/Q noncoherent correlator

represented as W/Δ, where W and Δ are the number of PN chips for the round-trip delay and search step size, respectively.

The system under consideration in this paper is the parallel acquisition using the single-dwell and double-dwell detection schemes for the access channel. Since the parallel acquisition is also implemented by a bank of N parallel I/Q noncoherent correlators as shown in Fig. 1, the number of test cells assigned to each I/Q noncoherent correlator is given by $V/N(=M)$. The structure of an I/Q noncoherent correlator is shown in Fig. 2. The parallel acquisition for the single-dwell and double-dwell detection schemes can be described as follows: First of all, the parallel acquisition for the single-dwell detection scheme is described. Defining the sample as the sum of I/Q noncoherent correlator outputs for the given postdetection integation(noncoherently summations) length L as shown in Fig. 1, the samples corresponding to all test cells in the uncer-

tainty region are compared. Finally, this scheme only selects the test cell(code-phase) that corresponds to the largest of V samples.

The double-dwell detection scheme consists of two separate modes, the search mode and the verification mode [3-7]. The search mode tests if the largest sample exceeds a decision threshold θ. If the test passes, the acquisition process moves to the verification mode ; otherwise, an acquisition attempt is done again within a given access channel preamble, namely, the new V samples are collected. The verification mode tests if n out of k samples for the selected code-phase exceed θ. If n out of k samples exceed θ, the acquisition is declared ; otherwise, the acquisition process returns to the search mode. In this paper, a decision threshold for two modes of the double-dwell detection scheme is the same. After the declaration of the initial acquisition, if a correct code-phase is inputted to the tracking process, the acquisition process terminates. But, if a false code-phase is inputted to the tracking process, and two detection schemes return to acquisition process after the false alarm penalty time, which is due to the size of an access channel message and the average random-delay D for the avoidance of the collision of an access channel slot.

C. Mean Acquisition Time

The acquisition model of the double-dwell detection scheme described above can be represented as the state diagram shown in Fig. 3.a. In Fig. 3.a, the expression of the required acquisition parameters and probabilities can be defined as follows :

S = size of an access channel slot.

N_w = number of PN chips corresponding to the coherent integration length.

T = number of acquisition attempts within a given access channel preamble in the double-dwell detection scheme.

T_d = dwell time of the double-dwell detection scheme as LN_wT_c.

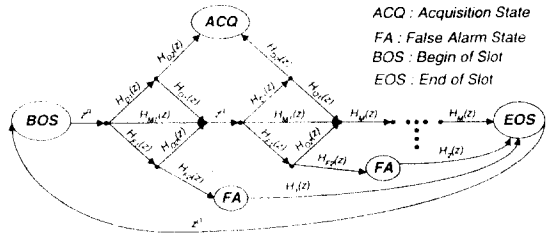

Fig. 3.a. State diagram of the double-dwell detection scheme

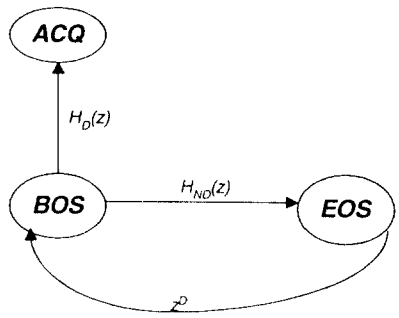

Fig. 3.b. Simplified state diagram

R = reset time for initialization.

I = number of all H_1 cells in the uncertainty region.

$P_{D_{1i}}$ = detection probability of H_{1i}(i-th H_1) cell in the search mode.

$P_{D_{2i}}$ = detection probability of H_{1i} cell in the verification mode.

P_{D_1} = detection probability of the search mode.

P_{M_1} = miss probability of the search mode.

P_{F_1} = false alarm probability of the search mode.

P_{F_2} = flase alarm probability of the verification mode.

The state diagram is used in deriving the moment generating function of the acquisition time owing to the Markovian nature of the acquisition process. In the state diagram of the double-dwell detection scheme shown in Fig. 3.a, $H_{D_1}(z)$, $H_{D_2}(z)$, $H_{M_1}(z)$, $H_{F_1}(z)$, $H_{F_2}(z)$, $H_{O_1}(z)$, $H_{O_2}(z)$, $H_M(z)$, $H_1(z)$, and $H_2(z)$ are given by

$$H_{D_1}(z) = \sum_{i=1}^{I} P_{D_{1i}} z^{MT_d} = P_{D_1} z^{MT_d}, \tag{1}$$

$$H_{D_i}(z) = P_{D_{2i}} z^{kT_d}, \qquad i = 1, 2, I, \tag{2}$$

$$H_{M_i}(z) = \prod_{i=1}^{I} (1 - P_{D_{1i}}) z^{MT_d} = P_{M_i} z^{MT_d}, \tag{3}$$

$$H_{F_1}(z) = P_{F_1} z^{MT_d}, \tag{4}$$

$$H_{F_2}(z) = P_{F_2} z^{kT_d}, \tag{5}$$

$$H_{O_i}(z) = (1 - P_{D_{2i}}) z^{kT_d}, \qquad i = 1, 2, \ldots, I, \tag{6}$$

$$H_{O_2}(z) = (1 - P_{F_2}) z^{kT_d}, \tag{7}$$

$$H_M(z) = z^R [H_{D_i}(z) H_{O_1}(z) + H_{M_i}(z) + H_{F_1}(z) H_{O_2}(z)], \tag{8}$$

$$H_1(z) = z^{S-(MT_d + kT_d + R)}, \tag{9}$$

and

$$H_2(z) = z^{S-2(MT_d + kT_d + R)}, \ or \ z^{S-\{2(MT_d + R) + kT_d\}}. \tag{10}$$

Referring to Fig. 3.a, the overall detection probability that passes the verification mode is given by $\sum_{t=0}^{T-1} [H_M(z)|_{z=1}]^t \sum_{i=1}^{I} P_{D_{1i}} P_{D_{2i}}$. Using the flow graph reduction method, the state diagram of Fig. 3.a can be simplified as Fig. 3.b. $H_D(z)$ and $H_{ND}(z)$ of Fig. 3.b are represented by

$$H_D(z) = \sum_{t=0}^{T-1} [P_{M_i} z^{MT_d} + \sum_{i=1}^{I} P_{D_{1i}} (1 - P_{D_{2i}}) z^{(M+k)T_d} + P_{F_1} (1 - P_{F_2}) z^{(M+k)T_d}]^t \cdot z^{(t+1)R} \sum_{i=1}^{I} P_{D_{1i}} P_{D_{2i}} z^{(M+k)T_d} \tag{11}$$

and

$$H_{ND}(z) = [P_{M_i} + \sum_{i=1}^{I} P_{D_{1i}} (1 - P_{D_{2i}}) + P_{F_1} (1 - P_{F_2})]^T z^S + P_{F_1} P_{F_2} \sum_{t=0}^{T-1} [P_{M_i} + P_{F_1} (1 - P_{F_2}) + \sum_{i=1}^{I} P_{D_{1i}} (1 - P_{D_{2i}})]^t z^S, \tag{12}$$

where $P_{D_i} + P_{M_i} + P_{F_i} = 1$ and $P_{D_i} = \sum_{i=1}^{I} P_{D_{1i}}$.

Since the single-dwell detection scheme has only one acquisition attempt within a given access channel preamble, $H_D(z)$ and $H_{ND}(z)$ of the single-dwell detection scheme in Fig. 3.b can be written as

$$H_D(z) = P_{D_s} z^{(MT_s + R)} \tag{13}$$

and

$$H_{ND}(z) = (1 - P_{D_s}) z^S, \tag{14}$$

where P_{D_s} is the detection probability and T_s is the dwell time represented by $LTN_w T_c$.

In (13), the detection probability P_{D_s} is based on the fact that the postdetection integration length of the single-dwell detection scheme is T times larger than that of the double-dwell detection scheme. Thus, the minimum size of an access channel preamble of the double-dwell detection scheme is represented as $T(MT_d + kT_d + R)$, while the minimum size of an access channel preamble of the single-dwell detection scheme is represented as $MT_s + R$.

Using Mason's gain formula, the transfer function for Fig. 3.b is given by

$$U(z) = \frac{H_D(z)}{1 - z^D H_{ND}(z)}, \tag{15}$$

where the transfer function $U(z)$ is the moment generating function. Thus, the mean acquisition time, $E[T_{ACQ}]$, is given by

$$E[T_{ACQ}] = \frac{d}{dz} \ln U(z) \Big|_{z=1} = \left[\frac{H_D'(1)}{H_D(1)} + \frac{(\frac{D}{S} + 1) H_{ND}'(1)}{1 - H_{ND}(1)} \right], \tag{16}$$

where $H_D'(1)$ and $H_{ND}'(1)$ are $\frac{d}{dz} H_D(z)\Big|_{z=1}$ and $\frac{d}{dz}$

$H_{ND}(z)\Big|_{z=1}$, respectively.

The acquisition probabilities can be obtained by substituting $z=1$ into $H_D(z)$ given by (11) and (13). Referring to (11), the acquisition probability of the double-dwell detection scheme is given by

$$P_{ACQ}=\sum_{i=1}^{J} P_{D_1} P_{D_2} \sum_{t=0}^{\tau-1} [P_{M_1} + \sum_{t=1}^{J} P_{D_1}(1-P_{D_2}) + P_{F_1}(1-P_{F_2})]^t. \quad (17)$$

From (13), the acquisition probability of the single-dwell detection scheme is given by

$$P_{ACQ}=P_{D_1}. \quad (18)$$

Ⅲ. Analysis of The Required Probabilities

A. Output Characteristic of The I/Q Noncoherent Correlator

In order to evaluate the acquisition performance, we consider the discrete multipath Rayleigh fading channel [10]. The discrete multipath intensity profile $\rho(\tau)$ of a fading channel as a function of the time delay τ can be modeled by

$$\rho(\tau)=\sum_{i=1}^{J} E[\alpha_i^2]\,\delta(\tau-\tau_i), \quad (19)$$

where α_i and τ_i are the path gain and the time delay of the i-th path, respectively. The path gains are independent and identically distributed Rayleigh random variables with mean square values $E[\alpha_i^2]$. The number of multipath components, J, is $[T_m/T_c]+1$, where T_m is the delay spread of a channel, and $[\cdot]$ denotes the integer part. In [9, 11], an access channel preamble of the k-th user can be represented as

$$S^{(k)}(t)=\sqrt{E_c^{(k)}}\cos w_c(t)\sum_n w_{0,n}^{(k)} a_{I,n}^{(k)} h(t-nT_c) = \sqrt{E_c^{(k)}}\sin w_c(t)\sum_n w_{0,n}^{(k)} a_{Q,n}^{(k)} h(t-nT_c), \quad (20)$$

where $a_{I,n}^{(k)}$ and $a_{Q,n}^{(k)}$ are the I and Q PN sequences, $w_{0,n}^{(k)}$ is the Walsh index 0 sequence, $E_c^{(k)}$ is the PN chip energy, and $h(t)$ is the impulse response of the band-limited filter.

The received signal in cellular DS/CDMA reverse link can be written as

$$r(t)=\sum_{i=1}^{N_u}\sum_{j=1}^{J} \alpha_j^{(i)}\sqrt{E_c^{(k)}}\,[\cos(w_c t-\varphi_j^{(i)}) \sum_n w_{s,n}^{(i)} a_{I,n}^{(i)} h(t-nT_c-\tau_j^{(i)})]+\sin(w_c t-\varphi_j^{(i)}) \sum_n w_{s,n}^{(i)} a_{Q,n}^{(i)} h(t-nT_c-\tau_j^{(i)})] + \sum_{m=1}^{N_c}\sum_{i=1}^{N_u}\sum_{j=1}^{J} \alpha_j^{(mi)}\sqrt{E_c^{(mi)}} [\cos(w_c t-\varphi_j^{(mi)}) \sum_n w_{s,n}^{(mi)} a_{I,n}^{(mi)} h(t-nT_c-\tau_j^{(mi)})] + \sin(w_c t-\varphi_j^{(mi)}) \sum_n w_{s,n}^{(mi)} a_{Q,n}^{(mi)} h(t-nT_c-\tau_j^{(mi)})] + \sqrt{2}\,n_I(t)\cos w_c t-\sqrt{2}\,n_Q(t)\sin w_c t, \quad (21)$$

where N_u and N_c are the number of users and the number of other cells, respectively, $\varphi_j^{(i)}$ is the random phase of the j-th path for the i-th user, $w_{s,n}^{(i)}$ is the Walsh index s sequence of the i-th user, and $n_I(t)$ and $n_Q(t)$ are lowpass Gaussian random processes with zero mean and a two-sided power spectral density $N_0/2$. The subscript m also denotes the component of other cell.

Referring to (21) and the I/Q noncoherent correlator of Fig. 2, Y_I and Y_Q of the k-th user in the home cell are represented as

$$Y_I=N_w\sqrt{E_c^{(k)}}\sum_{j=1}^{J}\alpha_j^{(k)}R(\lambda_j^{(k)})\cos\varphi_j^{(i)}+\sum_{n=1}^{N_w} n_{I,n} \quad (22)$$

and

$$Y_Q=N_w\sqrt{E_c^{(k)}}\sum_{j=1}^{J}\alpha_j^{(k)}R(\lambda_j^{(k)})\sin\varphi_j^{(k)}\sin\varphi_j^{(k)}+\sum_{n=1}^{N_w} n_{Q,n} \quad (23)$$

where $R(\lambda_j^{(k)})=\int|H(f)|^2\cos(2\pi f\lambda_j^{(k)})\,df$, $\lambda_j^{(k)}$ is the

timing error between the j-th path and code sequence of the local PN code generator, and N_w is the number of PN chips for a Walsh symbol duration. From(22) and (23), the variances of Y_I and Y_Q are given by $N_w I_o/2$. I_o is the interference spectral density that is due to background noise, multipath interference, multiple access interference, and other cells interference. To evaluate the interference on the reverse link, we assume that the number of users is the same in all cells and the users are uniformly distributed. Also, the independent fading of all users in all cells is assumed. Generally, the interference described above is treated as the additive Gaussian noise. In this case, the interference spectral density I_o for the h-th path of the k-th user can be represented as

$$I_o = N_o + E_c^{(k)}\{E[(\alpha_h^{(k)})^2]\sum_{\substack{n=-\infty \\ n\neq 0}}^{\infty} R^2(nT_c) + \sum_{\substack{j=1 \\ j\neq h}}^{J} E[(\alpha_j^{(k)})^2]\sum_{n=-\infty}^{\infty} R^2(nT_c) + \sum_{\substack{i=1 \\ i\neq k}}^{N_u} E_c^{(i)}\sum_{j=1}^{J} E[(\alpha_j^{(i)})^2]\sum_{n=-\infty}^{\infty} R^2(nT_c) + R_f\sum_{i=1}^{N_u} E_c^{(i)}\sum_{j=1}^{J} E[(\alpha_j^{(i)})^2]\sum_{n=-\infty}^{\infty} R^2(nT_c), \quad (24)$$

where R_f is the ratio of other cells user interference to home cell other user interference. Typical value for R_f is 0.55 [11]. I_o is also based on a implicit assumption which the phase $\varphi_j^{(k)}$ remains constant over the N_w chips accumulated.

B. Detection, False Alarm, and Miss Probabilities

To facilitate the derivation of the probability expressions, we shall adopt the following assumptions [8]: 1) all test statistics are independent, 2) there are IH_1 cells in the uncertainty region, 3) all test cells are a priori equally likely, 4) the output characteristics of the I/Q noncoherent correlator are analyzed for the fast fading model with Rayleigh-distributed envelope statistics.

The optimum decision method is the log-likelihood ratio test, but we can use the suboptimum decision method that compares the sample with a decision threshold θ under low E_c/I_o. In this case, if the decision variable η is the sum of the I/Q noncoherent correlator outputs Z_l, $l=1, 2, \ldots, L$, which are mutually independent, $2\eta/V_N$ under hypothesis H_0 is chisquare distributed with $2L$ degrees of freedom. Hence, the probability density function of η is given by

$$f_\eta(\eta|H_o) = \frac{1}{(L-1)!V_N^L}\ \eta^{L-1}\, e^{\frac{-\eta}{V_N}}, \quad (25)$$

where $V_N = N_w I_0$.

Using Y_I and Y_Q given by (22) and (23), the I/Q noncoherent correlator output means V_{F_i}, $i=1, 2, \ldots, I$ corresponding to H_{1i}, $i=1, 2, \ldots, I$ are represented by

$$V_{F_i} = N_w^2 E_c \sum_{j=1}^{J} E[\alpha_j^2]\, R^2(\lambda_{ij}) + N_w I_0, \quad i=1, 2, \ldots, I, \quad (26)$$

were α_j is the path gain of the j-th path and λ_{ij} is the timing error between the j-th path and code sequence of the local PN code generator corresponding to the H_{1i} cell. Using (26), the probability density function of η under hypothesis H_1 is given by

$$f_\eta(\eta|H_{1i}) = \frac{1}{(L-1)!V_{F_i}^L}\ \eta^{L-1}\, e^{\frac{-\eta}{V_{F_i}}}, \quad i=1, 2, \ldots, I. \quad (27)$$

Using the probability density functions of (25) and (27) above, we can derive the probabilities that are required in the search mode and the verification mode. Since the detection probability $P_{D_{1i}}$ corresponding to the H_{1i} cell in the search mode is the probability that the H_{1i} cell is larger than all $(V-1)$ cells and larger than θ, the detection probabilities $P_{D_{1i}}$, $i=1, 2, \ldots, I$ are represented as

$$P_{D_{1i}} = \int_\theta^\infty f_\eta(\eta|H_{1i})\left[\int_0^\eta f_x(x|H_0)\,dx\right]^{(V-I)} \prod_{\substack{l=1 \\ l\neq i}}^{I}\left[\int_0^\eta f_y(y|H_{1l})\,dy\right] d\eta, \quad i=1, 2, \ldots, I. \quad (28)$$

Since there are IH_1 cells within the uncertainty region,

the detection probability P_{D_1} of the search mode for the double-dwell detection scheme can be written as

$$P_{D_1}=\sum_{i=1}^{I}\int_{\theta}^{\infty}\frac{\eta^{LT-1}e^{\frac{-\eta}{V_{F_i}}}}{(L-1)!V_{F_i}^{LT}}\left[1-e^{\frac{-\eta}{V_N}}\sum_{n=0}^{LT-1}\frac{(\frac{\eta}{V_N})^n}{n!}\right]^{(W-I)}$$

$$\prod_{\substack{l=1\\l\neq i}}^{I}\left[1-e^{\frac{-\eta}{V_{F_l}}}\sum_{n=0}^{LT-1}\frac{(\frac{\eta}{V_{F_l}})^n}{n!}\right]d\eta. \quad (29)$$

Then, if the number of acquisition attempts for the double-dwell detection scheme is T within a given access channel preamble, referring to part C of section II, the detection probability P_D, of the single-dwell detection scheme is given by

$$P_{D_2}=\sum_{i=1}^{I}\int_{\theta}^{\infty}\frac{\eta^{LT-1}e^{\frac{-\eta}{V_{F_i}}}}{(L-1)!V_{F_i}^{LT}}\left[1-e^{\frac{-\eta}{V_N}}\sum_{n=0}^{LT-1}\frac{(\frac{\eta}{V_N})^n}{n!}\right]^{(W-I)}$$

$$\prod_{\substack{l=1\\l\neq i}}^{I}\left[1-e^{\frac{-\eta}{V_{F_l}}}\sum_{n=0}^{LT-1}\frac{(\frac{\eta}{V_{F_l}})^n}{n!}\right]d\eta. \quad (30)$$

The miss probability of the search mode is the probability that all samples are less than θ. Thus, the miss probability P_{M_1} of the search mode is given by

$$P_{M_1}=\left\{\prod_{i=1}^{I}\left[1-e^{\frac{-\theta}{V_{F_i}}}\sum_{n=0}^{L-1}\frac{(\frac{\theta}{V_{F_i}})^n}{n!}\right]\right\}$$

$$\left[1-e^{\frac{-\theta}{V_N}}\sum_{n=0}^{L-1}\frac{(\frac{\theta}{V_N})^n}{n!}\right]^{(W-I)}. \quad (31)$$

The false alarm probability of the search mode is given by

$$P_{F_1}=1-P_{D_1}-P_{M_1}. \quad (32)$$

The verification mode was described in B of section II, and the evaluation of its detection and false alarm probabilities is represented as follows: The detection probabilities $P_{D_{2i}}$, $i=1, 2, \ldots, I$ of the verification mode that correspond to H_{1i}, $i=1, 2, \ldots, I$ are given by

$$P_{D_{2i}}=\sum_{m=n}^{k}\binom{k}{m}P_{1i}^m(1-P_{1i})^{k-m}, \quad i=1, 2, \ldots, I, \quad (33)$$

where P_{1i} is the probability that the sampe of H_{1i} exceeds θ. Hence, P_{1i}, $i=1, 2, \ldots, I$ are represented by

$$P_{1i}=e^{\frac{-\theta}{V_{F_i}}}\sum_{n=0}^{L-1}\frac{(\frac{\theta}{V_{F_i}})^n}{n!}, \quad i=1, 2, \ldots, I. \quad (34)$$

The probability P_{F_2} that the false code-phase passes the verification mode is also given by

$$P_{F_2}=\sum_{m=n}^{k}\binom{k}{m}P_2^m(1-P_2)^{k-m}, \quad (35)$$

where P_2 is the probability that the sample of the H_0 cell exceeds θ. Using (25), P_2 is represented by

$$P_2=e^{\frac{-\theta}{V_N}}\sum_{n=0}^{L-1}\frac{(\frac{\theta}{V_N})^n}{n!}. \quad (36)$$

IV. Numerical Results

In evaluating the performance of two detection schemes, we consider the following parameters: the period of a PN chip $T_C=813.8$ns, Walsh symbol duration $T_W=208.33\mu$s, number of I/Q noncoherent correlators $N=6$, search step size $\Delta=1/2$, total search window length $W=148$ PN chips(cell radius = 20 km), reset time $R=1.25$ms, $k=4$ and $n=1$ for the verification mode of the double-dwell detection scheme. The average path powers $E[\alpha_i^2]$, $i=1, 2, \ldots, 6$ of the discrete multipath intensity profile considered in this paper are given by 0.5562, 0.2493, 0.1118, 0.0501, 0.0225, and 0.0101, respectively. The size of an access channel message is also fixed as 3 frames(60 ms).

Fig. 4 shows the acquisition probability for the thre-

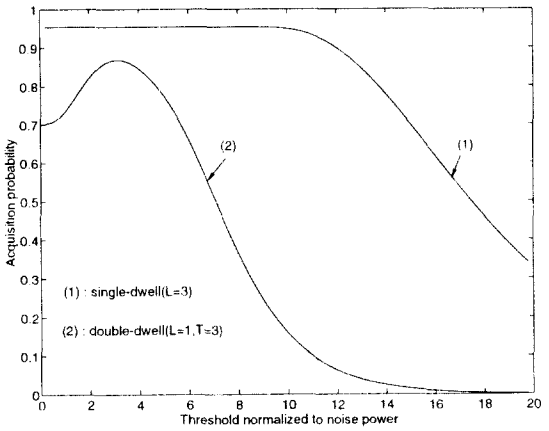

Fig. 4. Acquisition probability versus decision threshold for $E_S/I_o = 7$dB.

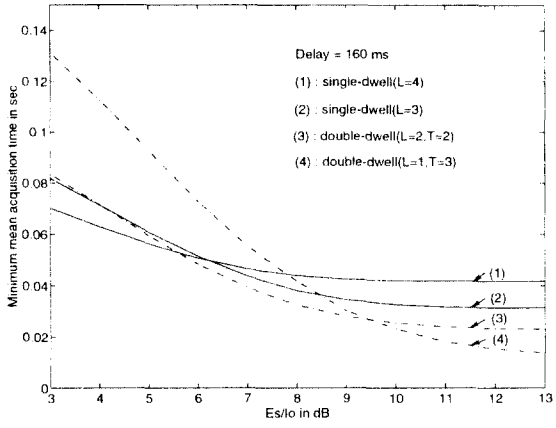

Fig. 6. Minimum mean acquisition time versus E_s/I_o for $D = 160$ms.

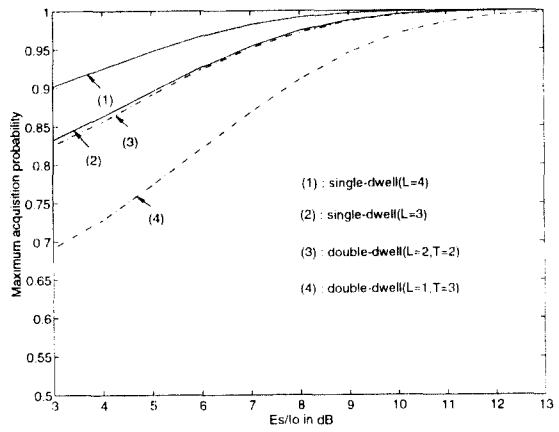

Fig. 5. Maximum acquisition probability versus E_s/I_o.

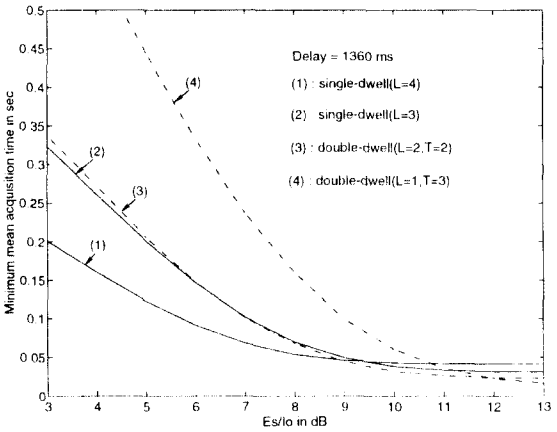

Fig. 7. Minimum mean acquisition time versus E_s/I_o for $D = 1360$ms.

shold setting at $E_S/I_O = 7$dB, where E_S is $N_W E_C$. The double-dwell detection scheme shows the maximum acquisition probability at $\theta = 3$. But, the single-dwell detection scheme shows the maximum acquisition probability at $\theta = 0$. In this figure, the double-dwell detection scheme needs to choose a decision threshold which shows the maximum acquisition probability, while the single-dwell detection scheme does not need to do it. In the double-dwell detection scheme, as the sensitivity of the acquisition time to changes in θ increases, the choice of an optimum decision threshold is very important.

Fig. 5 shows the maximum acquisition probabilities of the double-dwell and single-dwell detection schemes for various values of E_S/I_O. When an access channel preamble is similarly employed for two detection schemes, the single-dwell detection scheme shows larger acquisition probability than the double-dwell detection scheme. The acquisition probabilities of the single-dwell detection scheme of $L = 3$ and the double-dwell detection scheme of $L = 2$ and $T = 2$ are almost

the same. The results show that the method to increase the acquisition probability increases L more than T within a given access channel preamble.

Fig. 6 shows the minimum mean acquisition time with respect to E_S/I_O in the case of $D=160$ms, while Fig. 7 shows the minimum mean acquisition time with respect to E_S/I_O in the case of $D=1360$ms. Considering two figures, the sensitivity of the acquisition time with respect to E_S/I_O in two detection schemes is shown to increase as D increases. Then, in view of the sensitivity of the acquisition time to changes in D, the single-dwell detection scheme shows a better performance. This can be explained by the fact that sensitivity of the acquisition time to changes in D is influenced by the acquisition probabilities of two detection schemes.

V. Conclusion

This paper has considered the parallel acquisition performance for the single-dwell detection scheme and the double-dwell detection scheme in the cases of multiple H_1 cells and multipath fading channel. The mean acquisition time of two detection schemes has been derived to consider multiple H_1 cells. The results have demonstrated that the single-dwell detection scheme does not need to choose an optimum decision threshold. But, in order to minimize the acquisition time, the double-dwell detection scheme must choose an optimum decision threshold. When the size of an access channel preamble is similarly employed for two detection schemes, the single-dwell detection scheme shows both larger acquisition probability and smaller sensitivity of acquisition time to changes in D than double-dwell detection scheme. Two detection schemes proposed show a better performance in case that the acquisition probability is more than 0.95, then the single-dwell detection scheme requires shorter size of an access channel preamble than the double-dwell detection scheme in order that the acquisition probability is more than 0.95.

References

1. A. Polydoros and C. L. Weber, "A unified approach to serial search spread-spectrum code acquisition-part I: general theory," *IEEE Trans. Commun.*, vol. Com-32, pp. 542-549, May 1984.
2. K. S. Gilhousen, etc., "On the capacity of a cellular CDMA system," *IEEE Trans. Veh. Technol.*, vol. VT-40, pp. 303-312, May 1991.
3. A. Polydoros and C. L. Weber, "A unified approach to serial search spread-spectrum code acquisition-part II: a matched-filter receiver," *IEEE Trans. Commun.*, vol. Com-32, pp. 550-560, May 1984.
4. B. B. Ibrahim and A. H. Aghvami, "Direct sequence spread spectrum matched filter acquisition in frequency-selective Rayleigh fading channels," *IEEE J. Select. Areas in Commun.*, vol. SAC-12, pp. 885-890, June 1994.
5. L. B. Milstein, J. Gevargiz, P. K. Das, "Rapid acquisition for direct sequence spread-sprectrum communications using parallel SAW convolvers," *IEEE Trans. Commun.*, vol. Com-33, pp. 593-600, July 1984.
6. E. A. Sourour and S. C. Gupta, "Direct sequence spread spectrum parallel acquisition in a fading mobile channel," *IEEE Trans. Commun.*, vol. Com-38, pp. 992-998, July 1990.
7. E. A. Sourour and S. C. Gupta, "Direct sequence spread spectrum parallel acquisition in nonselective and frequency-selective Rician a fading channels," *IEEE J. Select. Areas in Commun.*, vol. SAC-10, pp. 535-544, April 1992.
8. Y. T. Su, "Rapid code acquisition algorithms employing PN matched filters," *IEEE Trans. Commun.*, vol. Com-36, pp. 724-733, June 1988
9. *TIA/EIA IS-95 Interim standard*, TIA, July 1993.
10. J. G. Proakis, *Digital communications*, Mcgraw-Hill: New York, 1989.
11. A. J. Viterbi, *CDMA principles of spread spectrum communication*, Addison-Wesley: New York, 1995.

康 法 周(Bub Joo Kang) 정회원

1983년 2월 : 경희대학교 전자공학과 졸업(공학사)
1985년 8월 : 연세대학교 대학원 전자공학과 졸업(공학석사)
1992년 3월~현재 : 연세대학교 대학원 전자공학과 박사과정
1988년 2월~현재 : 한국전자통신연구소 이동통신방식 연구실 선임연구원

李 亨 來(Hyung Rae Park) 정회원

1982년 2월 : 한국항공대학 전자공학과 졸업(공학사)
1985년 8월 : 연세대학교 대학원 전자공학과 졸업(공학석사)
1993년 12월 : Syracuse Univ(미) 전자공학과 졸업(공학박사)
1985년 9월~현재 : 한국전자통신연구소 이동통신방식 연구실 선임연구원

孫 廷 榮(Jung Young Son) 정회원

1973년 2월 : 한국항공대학 전자공학과 졸업(공학사)
1981년 12월 : 미국 University of Tennessee 전자공학과 졸업(공학석사)
1984년 12월 : 미국 University of Tennessee 응용과학과 졸업(공학박사)
1989년~현재 : KIST 책임연구원
1985년~1989년 : University of Tennessee space Institute 선임연구원
1973년~1977년 : KAIST 연구원

康 昌 彦(Chang Eon Kang) 정회원

현재 : 연세대학교 전자공학과 교수
한국통신학회 논문지 제20권 제1호 참조